APPLICATIONS OF
MODELLING AND SIMULATION
http://arqiipubl.com/ams eISSN 2600-8084 VOL 3, NO. 1, 2019, 39-54

Nonlinearity of Single Coupled Reinforced Concrete Shear Walls Supported on Two Columns

Amir A. EL-Fadeel[1*], Naser F. EL-Shafey[2] and Heba M. Issa[3]

[1]Misr Higher Institute for Engineering and Technology, Mansoura, Egypt
[2]Faculty of Engineering, Cairo University, Egypt
[3]R. C. Institute Housing & Building National Research Center, Egypt

[*]Corresponding author: amirabdelfadeel@gmail.com

Received 28 January 2019, Revised 19 February 2019, Accepted 20 February 2019.

Abstract: Reinforced concrete coupled shear walls supported on two columns can be used to resist lateral loads in high rise buildings specially if columns are at ground floors to satisfy architectural requirements such as parking space dimensions. The objective of this paper is to illustrate theoretically the lateral behaviour of shear walls, connecting beams, transfer beams and supporting columns in elastic and post elastic stage. Consequently, a case study is considered to give a better understanding of the behaviour of the coupled system. Moreover, a three-dimensional non-linear finite element analysis is carried out for 18 samples taking into consideration cracking, crushing of concrete and yielding of rebar. The governing equation, which represents the general solution of the proposed differential equation, is used to validate the outcomes up to elastic range. The results are reported as the effect of characteristic strength, stiffness ratio between columns and walls, reinforcement ratio, on the ultimate horizontal load capacity and the ductility of the entire system. The results demonstrate that stiffness ratio between shear walls and supporting columns was more crucial on the response of the coupled system rather than characteristic strength and the reinforcement ratio.

Keywords: Connecting beams behaviour; Coupled shear walls supported on columns; Earthquake; Non-linear finite element analysis; Transfer beam behaviour.

1. INTRODUCTION

Coupled shear walls may be used to enhance the lateral resistance for the high rise building. However, architectural requirements may dictate that shear walls are discontinued in the first story to provide large open areas for entrance foyers or for parking requirements. The coupled shear walls may then be supported at first floor level on a set of columns or on a portal frame. This system contains shear walls which are dominated by flexural behaviour, and frames which are dominated by its shear deformation. Therefore, the whole behaviour of this system is a hybrid of flexural and shear deformation.

Morgan [1] studied seven stories coupled shear walls supported on columns under vertical loads only. This study included material linearity and non-linearity of two dimensional reinforced concrete structures under the action of monotonically increased loads. This study based on finite element analysis by using of Nonlinear Analysis of Reinforced Concrete and Shells (NARCS10) program. The finite element analysis by NARCS10 program included iso-parametric quadrilateral element, and steel reinforcement was modeled using two nodes discrete bar element as well as smeared steel element. It concluded that a transfer beam must have a height not less than 20% of the clear span of the lower wide floor, increasing or decreasing the amount of main steel of this type of structures has inconsequential effect on the ultimate load of the wall. This means that, the failure of the wall is mainly controlled by the ultimate compressive strength of concrete, and the use of 4, 5 and 6 nodes quadrilateral elements gives reasonable accuracy for the results.

Khaled [2] studied the same system of Morgan [1] using a finite element program, ANSYS. Additionally, pushover analysis was taken into account along with the effect of stiffness variation of columns, coupling beams, transfer beams and link beams. Moreover, scrutinised the load path-dependence for gravitational and pushover combinations. It concluded that the stress concentration pattern significantly differs depending on the type of loading. Geometric discontinuity regions capture the highest damage evolution rate. For example, under gravitational loading stress concentration takes place at the column-wall junction and also in the transfer and the link beams. On the other hand, for lateral loading the highest tensile stresses occur

at the column-wall junction of the loaded side and in coupling beams. Redistribution of stresses is evident through the course of loading with emphasis to the relative column to coupled shear wall stiffness. In turn, the position of the maximum bending stresses shifts from the base upwards with the progress of loading.

The main objective of the present work is to provide several parameters required to have a better understanding on the behaviour of the coupled shear walls supported on columns under quasi-static loading. The objectives can be summarised as follows: (1) Understanding the behavior of the coupled system taking into consideration the effect of material nonlinearity in vertical loading besides static pushover analysis. (2) Analysing the response of the coupled system on the ultimate horizontal load capacity, the ductility of the whole system under the effect of characteristic strength, stiffness ratio between columns and walls and the reinforcement ratio.

2. CASE STUDY

2.1 Geometrical Dimensions

The assumed dimensions of different structural elements are as follows: Plan area (20 × 30 m); Shear wall cross-section (0.5 × 4 m); Columns cross-section (0.5 × 1.5 m); Connecting beams cross-section (0.5 × 0.6 m); Transfer beam cross-section (0.5 × 1.5 m). The plan and elevation of the case study are shown in Figure 1.

2.2 Vertical and Horizontal Loads

Factored vertical loads were calculated due to weight of walls, coupling beams, columns, in addition to loads from the weight of slabs, where live load = 4 kN/m^2, superimposed dead load = 1.5 kN/m^2, weight of brick walls = 1.5 kN/m^2 and thickness of slabs = 220 mm. Additionally, distributed vertical loads/story = 100 kN/m. Horizontal loads are calculated by the simplified response spectrum analysis using ECP-203 [3], in which horizontal loads were distributed by the inverse of triangle with a maximum value, 500 kN, at the top floor level as shown in Figure 2. Vertical and horizontal loads were calculated as shown in Appendix.

2.3 Proposed Reinforcement

To predict the amount of steel ratio, finite element program SAP2000 was used to simulate the multi-story frame of the coupled shear walls system. The calculated straining actions were used to design the critical sections according to ECP-203 [3]. There are three collections of steel reinforcement for the whole structural elements as illustrated in Table 1. The distribution of steel reinforcement of Collection 3, as an example, can be illustrated as shown in Figure 3.

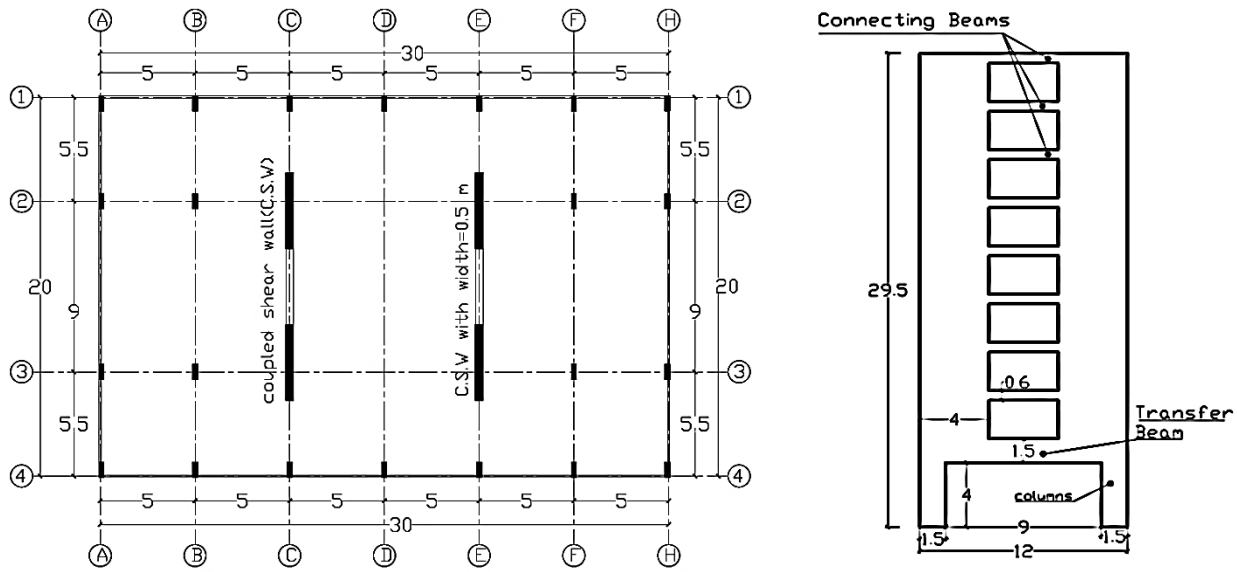

Figure 1. Plan and elevation of the coupled shear walls supported on columns

Table 1. Steel ratio for the three collections of reinforcement

Collection	Structural Member			
	Column (%)	Transfer beam (%)	Walls (%)	Connecting beams (%)
1	0.8	0.68	0.62	0.92
2	0.8	6.5	0.62	0.92
3	3.7	6.5	1.17	3.9

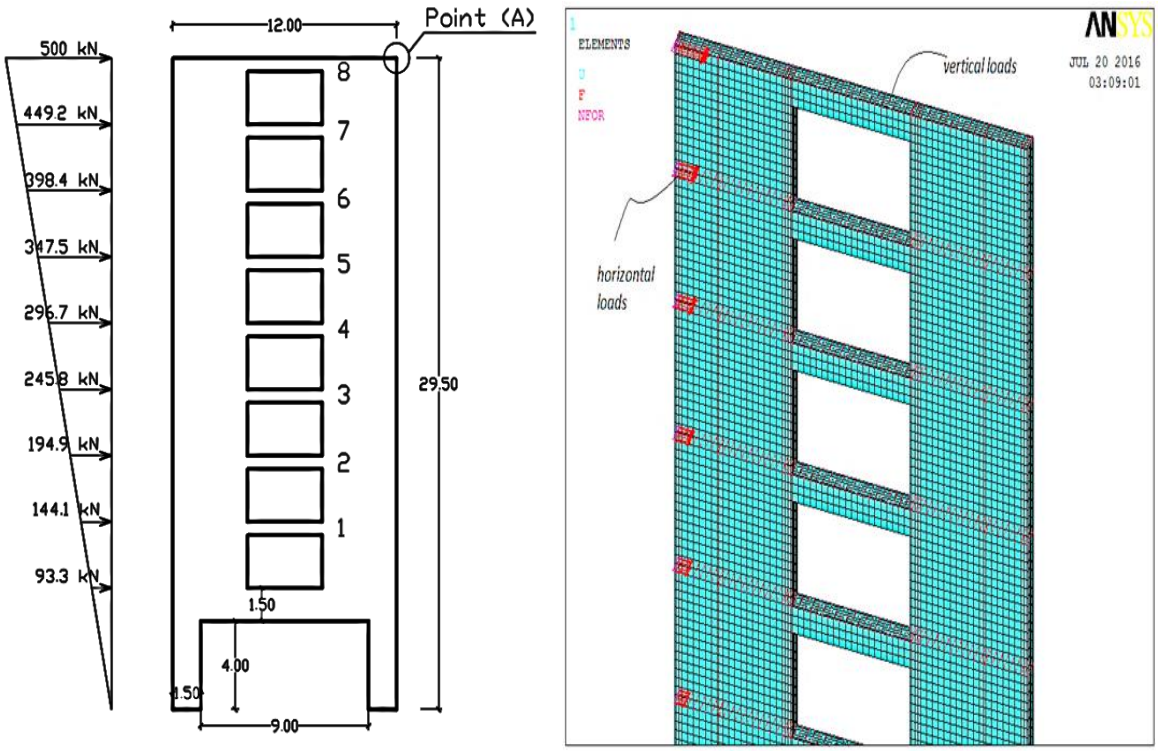

Figure 2. Equivalent horizontal loads applied on coupled shear walls system

2.4 Ductility

Ductility is the capability of the material/member to endure deformation beyond the elastic limit. To evaluate the ductility, the deformation may be strain, curvature, displacement or rotation. According to Pam et al. [4] and Kassem et al. [5], it is advisable to express the ductility in terms of a dimensionless ductility factor (μ) as shown in Equation (1).

$$\mu = \left[\frac{\Delta max}{\Delta y}\right] \tag{1}$$

where Δmax is the maximum deformation, at which the crushing of concrete for any structural member occurs, and Δy is the yielding deformation, at which the reinforcement for any structural element yields.

2.5 Main Parameters

The main parameters taken into consideration are listed in Table 2.

Table 2. Main parameters of the case study

Sample Number	Main Parameters					
	Comp. strength (MPa)	Reinforcement ratio (%)				Stiffness ratio between column and wall
		Column	Transfer Beam	Wall	Connecting Beam	
1	35	0.8	0.68	0.62	0.92	37.5
2	35	0.8	6.5	0.62	0.92	37.5
3	35	3.7	6.5	1.17	3.9	37.5
4	35	0.8	0.68	0.62	0.92	51.25
5	35	0.8	6.5	0.62	0.92	51.25
6	35	3.7	6.5	1.17	3.9	51.25
7	45	0.8	0.68	0.62	0.92	37.5
8	45	0.8	6.5	0.62	0.92	37.5
9	45	3.7	6.5	1.17	3.9	37.5
10	45	0.8	0.68	0.62	0.92	51.25
11	45	0.8	6.5	0.62	0.92	51.25
12	45	3.7	6.5	1.17	3.9	51.25
13	60	0.8	0.68	0.62	0.92	37.5
14	60	0.8	6.5	0.62	0.92	37.5
15	60	3.7	6.5	1.17	3.9	37.5
16	60	0.8	0.68	0.62	0.92	51.25
17	60	0.8	6.5	0.62	0.92	51.25
18	60	3.7	6.5	1.17	3.9	51.25

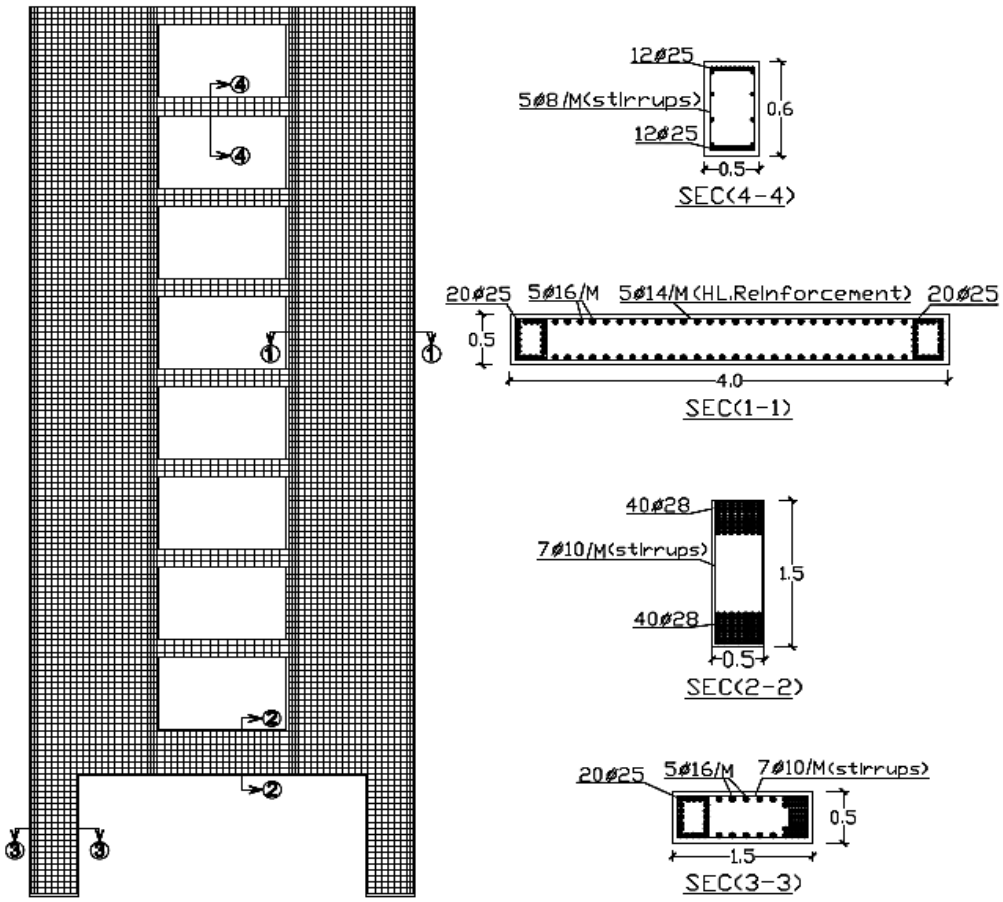

Figure 3. The distribution of steel reinforcement of collection (3) in the different structural elements.

3. PROPOSED GOVERNING EQUATION

In order to check if the model developed in the software is correct, it is very important to validate the results obtained. Because of the lack of experimental studies carried out on such system, approximating equation developed by Coull and Smith [6] is used to calculate the drift at point (A), which is illustrated in Figure 2. This equation is valid up to elastic range and it is depended on the geometry of the system and the case of applied lateral loads.

3.1 Calculation for $k\alpha H$

The value of $k\alpha H$ will define the degree of composite action and will indicate the mode of resistance to applied lateral loads. Therefore, it must be calculated at first before substituting into the governing equation. The general equation for calculating $k\alpha H$ is shown in Equation (2).

$$k\alpha H = \left[\frac{12 I_e l^2}{b^3 h I}\left(1 + \frac{AI}{A_1 A_2 l^2}\right) H^2\right]^{\frac{1}{2}} \tag{2}$$

where

$$k = \sqrt{\left[1 + \frac{AI}{A_1 A_2 l^2}\right]}$$

$$\alpha = \sqrt{\frac{12 I_e l^2}{b^3 h I}}$$

$$I_e = \frac{I_b}{1 + r}$$

$$r = \frac{12 E I_b}{b^2 G A}\lambda$$

According to Smith and Coull [6] and based on the calculated value of $k\alpha H$, the present system can be categorised as a coupled shear walls.

3.2 Calculation of Drift at Point (A)

The governing Equation (3), which represents the general solution of the proposed differential equation developed by Smith and Coull [6], is used to calculate the drift at point (A). It may be used only to give a solution up to elastic range without taking into consideration the non-linear behavior of concrete and rebar. The results obtained from that equation are compared with finite element program results within the elastic limit. Attaining the first cracks may be regarded as the end of the elastic stage.

$$\frac{EI}{WH^4} y = \frac{1}{24}\frac{k^2 - 1}{k^2}\left|\left(\frac{z}{H}\right)^4 - 4\left(\frac{z}{H}\right)^3\right| + \frac{1}{2(k\alpha H)^2}\left|\frac{k^2 - 1}{k^2} + \frac{1}{2}(\alpha H)^2(k^2 - 1) - 1\right|\left(\frac{z}{H}\right)^2 + C_1 + C_2\left(\frac{z}{H}\right) + C_3 \sinh(k\alpha z) + C_4 \cosh(k\alpha z) \tag{3}$$

where

$$C_1 = \frac{r_H r_1}{(k\alpha H)^2} - \frac{1}{k^2 (k\alpha H)^4}\operatorname{sech}(k\alpha H) + |\tanh(k\alpha H) + r_H r_L k^2 (k\alpha H)| C_3$$

$$C_2 = \frac{r_1}{(k\alpha H)^2} + (k^2 r_L - 1)\, k\alpha H C_3$$

$$C_3 = \frac{1}{\triangle}\left\{\frac{1}{(k\alpha H)^2}\left|\frac{1}{k^2}(\operatorname{sech}(k\alpha H) - 1) + \frac{1}{2}(\alpha H)^2(k^2 - 1)\right| - \frac{1}{k^2} r_1 - \frac{1}{2}(1 - r_L) + r_H r_L\right\}$$

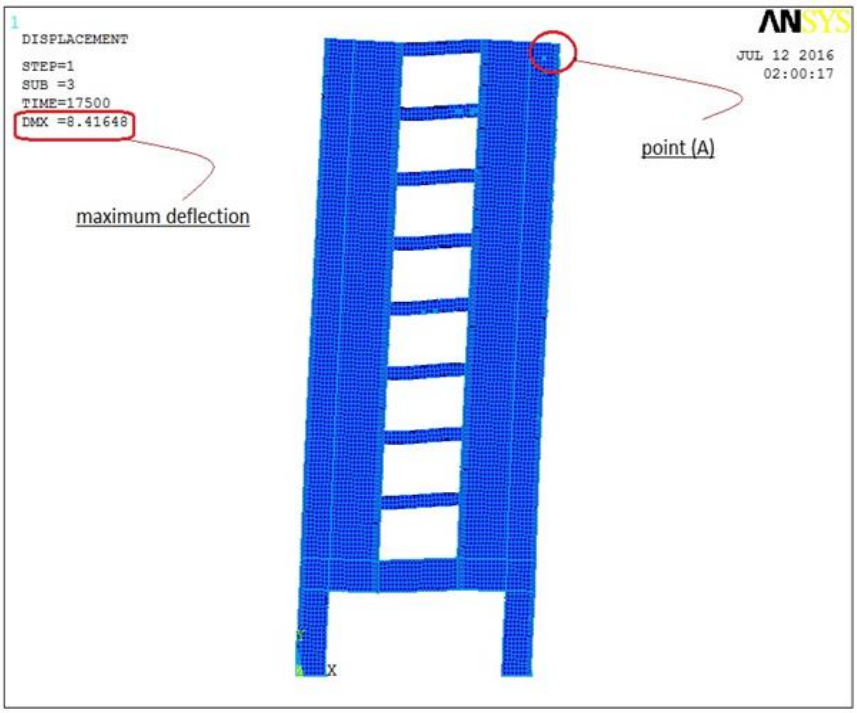

Figure 4. Maximum displacement of point (A) at which the first cracks occurred

$$C_4 = \frac{1}{k^2(k\alpha H)^4}\operatorname{sech}(k\alpha H) - C_3 \tanh(k\alpha H)$$

$$\triangle = (k\alpha H)^2(k\alpha H\, r_1 + \tanh(k\alpha H))$$

$r_H = 0.0, r_L = 1,$ according to Smith and Coull [6].

$$r_1 = \frac{I_o\, h}{I_c\, H}$$

By using the equations, the value of drift (y) at point (A) can be obtained as 10.29 mm.

3.3 Calculation of Drift at Point (A) using ANSYS14

Finite element program, ANSYS14 can be used to calculate the drift at point (A) at the end of elastic stage, in which the first cracks are occurred. The displacement at point (A) equals 8.41 mm according to the results obtained, as shown in Figure 4. By comparing the results of the two cases the difference was 1.87 mm, which may be considered well up to 20% difference.

4. FINITE ELEMENT ANALYSIS

The finite element analysis using ANSYS14 [7] package can be used to closely forecast the behaviour of the coupled system which subjected to in-plane forces. The load-deflection behaviour, crack propagation, first crack load, failure load, and failure mode can be predicted using the finite element method with an accuracy that is acceptable for engineering purposes. Furthermore, the program accounts for: (1) Material non-linearity of both concrete and steel, (2) Biaxial failure surface of concrete, (3) Nonlinear stress-strain curve of steel and (4) Concrete cracking and crushing.

4.1 Material Properties

4.1.1 Concrete

Concrete in compression: The idealised stress strain curve as in ECP-03 [3] was used for representing the actual behaviour of concrete in compression. It consists of a parabola up to a strain of 0.002 and straight horizontal line up to a strain of 0.003.

Concrete in tension: The tensile strength of concrete is very low and it might be generally about 10% of its compressive strength for normal concrete, but the tensile strength of high strength concrete can be calculated from Equation (4) according to Martinez et al., [8]. In this study, concrete was assumed as a linear elastic-brittle material in tension, and this is an essential factor causing the nonlinear behavior. Cracks are assumed to form in planes perpendicular to the direction of maximum principal tensile stress as soon as this reaches the specified concrete tensile strength.

$$f'_{sp} = 0.59\sqrt{f'_c} \tag{4}$$

The SOLID65 element: A concrete 3D-solid element was used to model the behaviour of the concrete with reinforcing bars which requires linear isotropic and multi-linear isotropic material properties to properly model for concrete. The multi-linear isotropic material uses the Von-Mises failure criterion along with the Willam and Warnke [9] model to define the failure of the concrete. "EX" is the initial tangent modulus of elasticity of the concrete (Ec) and "PRXY" is the Poisson's ratio (ν). The Young's modulus for normal concrete (concrete with compressive strength less than (41 MPa) approximately) is depended on Equation (5), and the Young's modulus for high strength concrete (concrete with compressive strength in excess (41 MPa) roughly) is depended on Equation (6) defined by Martinez et al. [8].

$$E_c = 4700\sqrt{f'_c} \tag{5}$$

$$E_c = 3320\sqrt{f'_c} + 6900 \qquad (\text{for } 21 \text{ MPa} < f'_c < 83 \text{ MPa}) \tag{6}$$

where a value of f'_c equal to a cylinder compressive strength in MPa units, and Poisson's ratio was assumed to be 0.2 for concrete. The uniaxial compressive stress-strain relationship for the concrete model was obtained using Equations (7)-(9) to calculate the multi-linear isotropic stress-strain curve for the concrete in compression Wight and Macgregor [10] and these equations are used in the present study:

$$f = \frac{E_c \varepsilon_c}{1 + \left(\frac{\varepsilon_c}{\varepsilon_o}\right)^2} \tag{7}$$

$$\varepsilon_0 = \frac{2f'_c}{E_c} \tag{8}$$

$$E_c = \frac{f}{\varepsilon_c} \tag{9}$$

where f is the stress at any strain ε_c and ε_o is the strain at the cylinder compressive strength f'_c. The multi-linear isotropic stress-strain curve, demands the first point of the curve to be entered by the user and it must satisfy Hooke's Law. The model that capable of predicting failure of concrete material is shown in Figure 5. The multi-linear curve is used to help for the convergence of the nonlinear solution algorithm as shown in Figure 6. Both cracking and crushing failure modes are taken into consideration. The two input strength parameters i.e., ultimate tensile and compressive strengths are demanded to define a failure surface of the concrete. Willam and Warnke [9] criterion is used to predict the failure of the concrete due multi-axial stress state.

In concrete element, cracking occurs when the principal tensile stress in any directions lies outside the failure surface. After cracking, the Young's modulus of concrete element is set to zero in the direction parallel to the principal tensile stress direction. Crushing takes place when all principal stresses are compressive and lie outside the failure surface. Thereafter, the Young's modulus is set to zero in all directions, and the element effectively disappears. For the implementation of the criterion of Willam and Warnke [9], material model in ANSYS14 [7] requires defining nine constants as shown in Table 3.

4.1.2 Steel Reinforcement

The Link 8-3D element is used to model the steel reinforcement. This element is a uniaxial tension-compression element. The mechanical properties of steel are well-known and understood. Steel is homogeneous and has usually the same yield strength in tension and compression. In the present study reinforcing steel is modeled as a bilinear elasto-plastic material using the idealised stress-strain curve as shown in Figure 7.

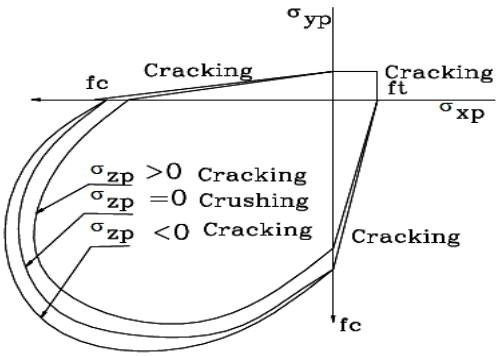

Figure 5. Failure surface of the concrete

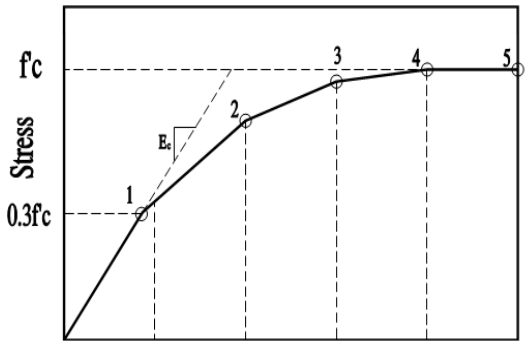

Figure 6. Idealised stress-strain curve for concrete in compression

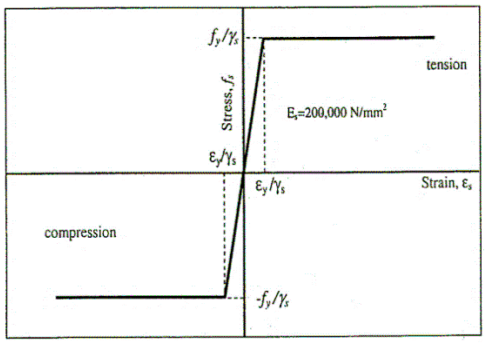

Figure 7. Idealised stress-strain curve for steel reinforcement

4.2 Material Modeling

The material models for SOLID65 and LINK8 Element, which were used in the finite element analysis using ANSYS14, are illustrated in Table 3. To obtain good results from the SOLID65 element, the use of a rectangular mesh is recommended. Therefore, the mesh was created as square or rectangular elements as shown in Figure 8. The volume sweep command was used to mesh the whole coupled system. The meshing of the reinforcement is a special case compared to the volumes. No mesh of the reinforcement is needed, because individual elements were created in the modelling through the nodes created by the mesh of the concrete volume. However, the necessary mesh attributes need to be set before each section of the reinforcement is created. The finite element model had exactly 84087 total numbers of elements consists of 49052 SOLID65, and 35035 LINK8. The boundary conditions were exactly simulated as a fixed support in which horizontal, vertical and rotational movements are restrained.

4.3 Modeling of Coupled Shear Walls Supported on Columns by ANSYS Program

Modeling of the coupled shear walls system was carried out where the node points of the solid elements coincide with the actual reinforcement locations as shown in Figure 8.

5. PUSHOVER ANALYSIS AND RESULTS

Lateral loads represent one of the significant concerns in high-rise buildings. Figure 9 shows the variation of top drift for all samples at different increments of loading. Apparently, the trend is nearly linear along the height at low load levels. However, at higher load increments, the drift at higher stories considerably differs and the trend tends to be non-linear.

To illustrate the steps of loading as well as understanding the behavior of the coupled system, sample 12 was taken as an example. At the beginning of loading, the structure was deformed until first flexure cracks were taken place at load 137.5 kN, therefore, this load was considered to be the first crack load (Pcr). At load 237.5 kN, first shear cracks occurred along with increasing in flexural cracks propagation. By increasing the loading rate to 575 kN, which is considered the yielding load (py) because of the beginning of yielding for stirrups of transfer beam, the drift value at the top point was observed equal to 57.99 mm (Δy) alongside forming of the first plastic hinge at connecting beam no.4, which is counted from the top floor as shown in Figure 10(a). According to Coull and Choo [11], it is assumed that the plastic hinge forms at the middle third of the height of the coupled system. Consequently, the elastic range is considered to be ended and the post-elastic range is begun.

Table 3: Material models for SOLID65, LINK8 element

<table>
<tr><th>Material Model No</th><th>Element Type</th><th>Material Properties</th></tr>
<tr><td>1</td><td>SOLID65</td><td>
<table>
<tr><th colspan="2">Linear Isotropic</th></tr>
<tr><td colspan="2">Elasticity Modulus, EX, is equal to $\left(\frac{f_1}{\varepsilon_1}\right)$ at point (1) at the curve.</td></tr>
<tr><td colspan="2">Poisson’s Ratio, PRXY, is equal to 0.20.</td></tr>
</table>
<table>
<tr><th>Multi-linear Isotropic</th></tr>
<tr><td>Five coordinates are needed to represent the stress-strain curve for concrete, Figure 2.</td></tr>
</table>
<table>
<tr><th colspan="2">Concrete</th></tr>
<tr><td>Open Shear Transfer Coefficient</td><td>0.2</td></tr>
<tr><td>Closed Shear Transfer Coefficient</td><td>0.9</td></tr>
<tr><td>Uniaxial Cracking Stress (Modules of rupture)</td><td>The concrete tensile strength f_t is typically 8% - 15% of the compressive strength and taken equal to 10% for normal concrete, and according to Equation (2).</td></tr>
<tr><td>Uniaxial Crushing Stress</td><td>The crushing stress value is taken from the stress-strain curve.</td></tr>
<tr><td>Biaxial Crushing Stress</td><td>0</td></tr>
<tr><td>Hydrostatic Pressure</td><td>0</td></tr>
<tr><td>Hydro Biaxial Crush Stress</td><td>0</td></tr>
<tr><td>Hydro Uniaxial Crush Stress</td><td>0</td></tr>
<tr><td>Tensile Crack Factor</td><td>0</td></tr>
</table>
</td></tr>
<tr><td>2</td><td>LINK8</td><td>
<table>
<tr><th>Linear Isotropic</th></tr>
<tr><td>Elasticity Models, EX, is equal to 2×10^5 MPa.</td></tr>
<tr><td>Poisson’s Ratio PRXY, is equal to 0.30.</td></tr>
</table>
<table>
<tr><th>Bilinear Isotropic</th></tr>
<tr><td>Yield Stresses follow the design material properties used for the experimental investigation.</td></tr>
<tr><td>Tangent Modulus is taken equal to Yield Stress.</td></tr>
</table>
</td></tr>
</table>

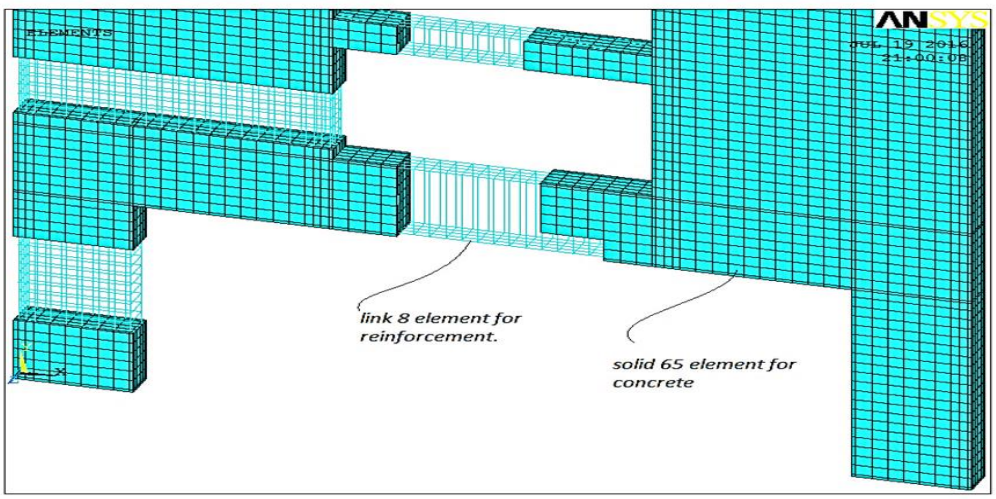

Figure 8. Modelling of the coupled shear walls system using ANSYS

By using the vector mode option of ANSYS14 [7], it was observed the regions of stress concentrations for the three principles stress at failure load as shown in Figure 11. These principle stresses are defined by Timoshenko and Goodier [12]. The first principle stress represents a maximum value (tension zone), and the third principle stress represents a minimum value (crushing zones). It was also found that further increasing of the loading rate may lead to the second plastic hinge at load 650 kN, which is considered to be the failure load (Pu) because of the crushing of concrete for the supporting columns as shown in Figure 10(b). At this load, it was also spotted the crushing of concrete for the transfer beam at the junction between connecting beams and the shear walls as shown in Figure 12. In addition, the maximum drift (Δmax) was noticed equal to 71.46 mm.

The main results for all samples are summarised in two main groups as shown in Tables 4 and 5. Group one includes samples number 1, 2, 3, 7, 8, 9, 13, 14, and 15 with stiffness ratio of 37.5% between columns and walls. Group two includes samples number 4, 5, 6, 10, 11, 12, 16, 17, and 18 with stiffness ratio of 51.25%. Nonlinearity besides variation of characteristic strength both influence on the deformation pattern and the top drift value. Figure 13(a) shows the horizontal load versus top drift relationship for samples 6, 12 and 18. They have the same stiffness and reinforcement ratio, except for the characteristic strength which varies from 35, 45, to 60 MPa, respectively. Furthermore, it was observed that maximum horizontal load capacity rises with the increasing of characteristic strength. In contrast, the top drift decreases with the increasing of characteristic strength. Figure 13(b) demonstrates the yielding and ultimate horizontal loads with their yielding and ultimate drifts, respectively. It can also estimate the ductility of each sample, as well as understanding which sample is more ductile. It was noticed that sample 6 is more ductile with respect to the other two samples.

It can also understand the behaviour of the coupled system if the stiffness ratio between columns and walls varies. Figures 14(a) and 14(b) show the horizontal load versus top drift relationship for samples 15 and 18. They have the same characteristic strength and reinforcement ratio, except for the stiffness ratio between shear walls and supporting columns which varies from 37.5% to 51.25%. The ultimate horizontal load capacity is increased by one third its value when the stiffness ratio is increased from 37.5% to 51.25%. In contrast, the ductility is decreased by about its half value when the stiffness ratio is increased.

Moreover, the coupled system response is affected by the variation of steel reinforcement ratio. Figure 15 depicts the horizontal load versus top drift relationship for samples 10, 11 and 12. They have the same characteristic strength and stiffness ratio, except for the reinforcement ratio which varies from collection one, two to collection three. It might attain a high ultimate capacity by utilising the collection three of reinforcement, but the ductility, in this case, may decrease to 1.23%. Generally, the ultimate horizontal load capacity and the ductility ratio, mainly governed by the stiffness ratio between shear walls and supporting columns rather than characteristic strength and the reinforcement ratio.

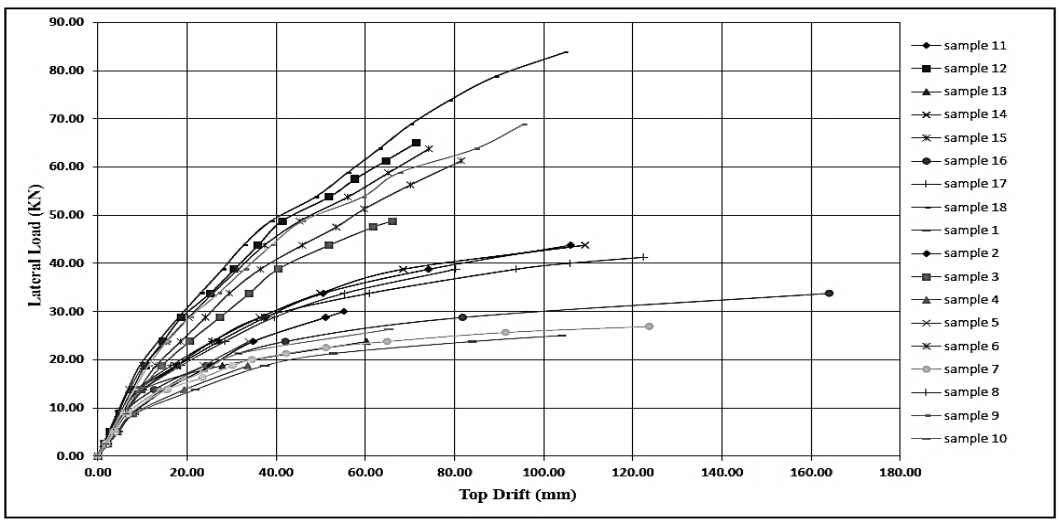

Figure 9. The variation of top drift for all samples at different increments of loading

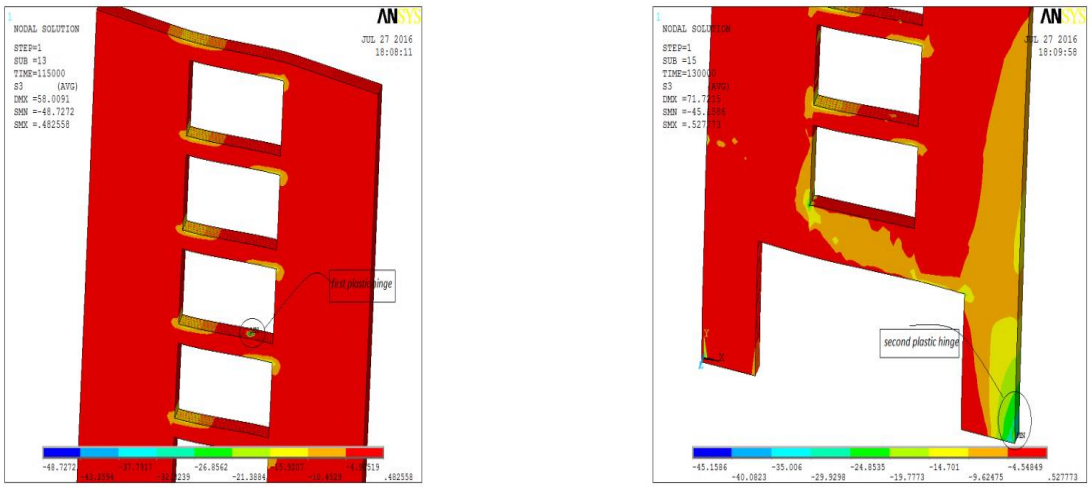

(a) First plastic hinge (b) Second plastic hinge

Figure 10. Plastic hinge for sample 12

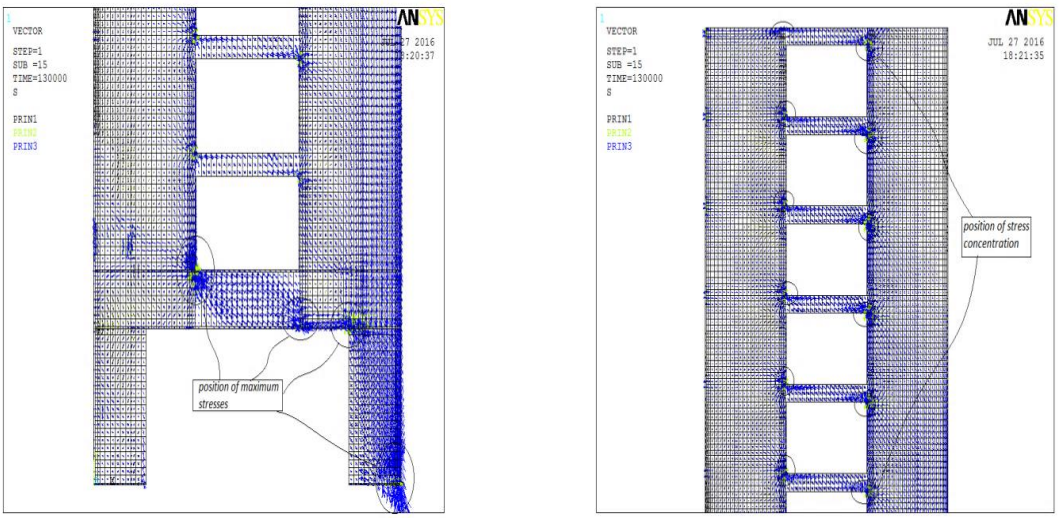

Figure 11. Principles stresses at failure load for sample 12

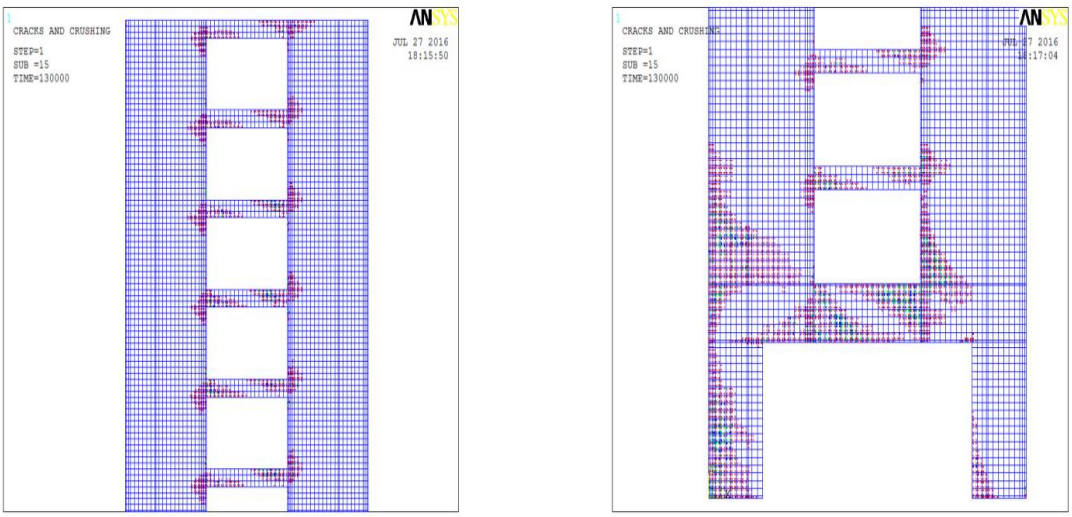

Figure 12. Crack pattern at failure load for sample 12

Table 4. Results of group one

	Sample Number	Pcr (ton)	Pv (ton)	Py (ton)	Pu (ton)	Yielding drift (mm)	Max. Drift (mm)	fcu (MPa)	Ductility (%)
Group one	1	8.75	13.75	13.75	25	21.93	104.22	35	4.75
	2	8.75	13.75	23.75	30	35.09	55.45	35	1.58
	3	13.75	18.75	38.75	48.75	40.59	66.26	35	1.63
	7	8.75	13.75	13.75	26.88	15.69	124.03	45	7.91
	8	8.75	18.75	23.75	38.75	28.68	80.49	45	2.81
	9	13.75	23.75	33.75	58.75	27.16	67.67	45	2.49
	13	8.75	13.75	18.75	23.75	28.04	60.37	60	2.15
	14	8.75	18.75	28.75	43.75	36.49	109.5	60	3.00
	15	13.75	23.75	33.75	63.75	25.89	74.28	60	2.87

Table 5. Results of group two

	Sample Number	Pcr (ton)	Pv (ton)	Py (ton)	Pu (ton)	Yielding drift (mm)	Maxim. Drift (mm)	fcu (MPa)	Ductility ratio (%)
Group two	4	8.75	13.75	13.75	18.75	19.52	33.64	35	1.72
	5	8.75	13.75	23.75	23.75	34.81	34.81	35	1.00
	6	13.75	23.75	51.25	61.25	60.02	81.51	35	1.36
	10	8.75	13.75	13.75	26.25	14.22	65.28	45	4.59
	11	8.75	18.75	23.75	43.75	27.33	106.05	45	3.88
	12	13.75	23.75	57.5	65	57.99	71.46	45	1.23
	16	8.75	13.75	18.75	33.75	24.31	164.06	60	6.75
	17	8.75	18.75	28.75	41.25	36.84	122.45	60	3.32
	18	13.75	23.75	73.75	83.75	78.99	104.66	60	1.32

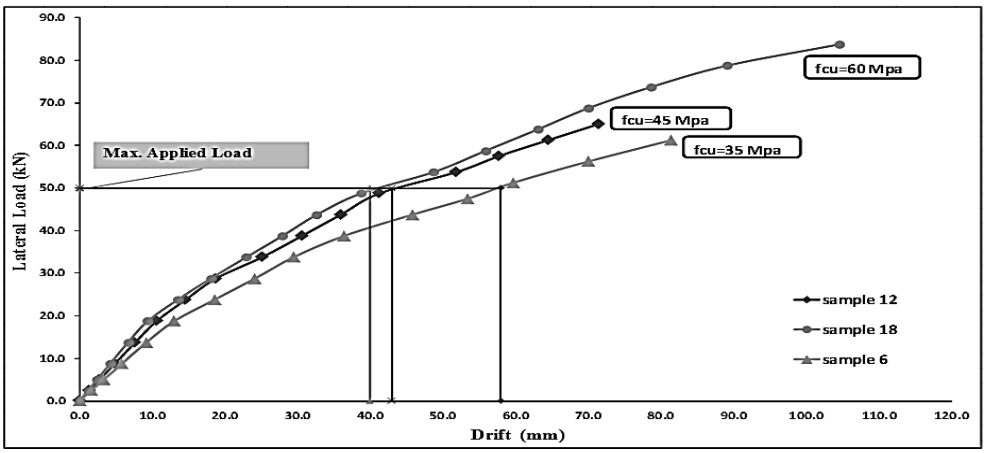

(a) The differences in the top drift value at the maximum applied horizontal load

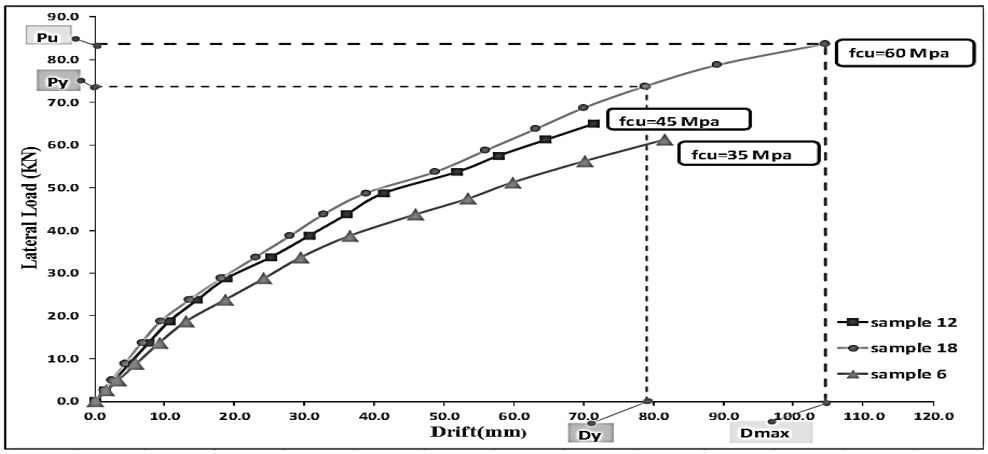

(b) The differences in the ductility ratio

Figure 13. The variation of top drift for samples 6, 12 and 18 at different increments of loading

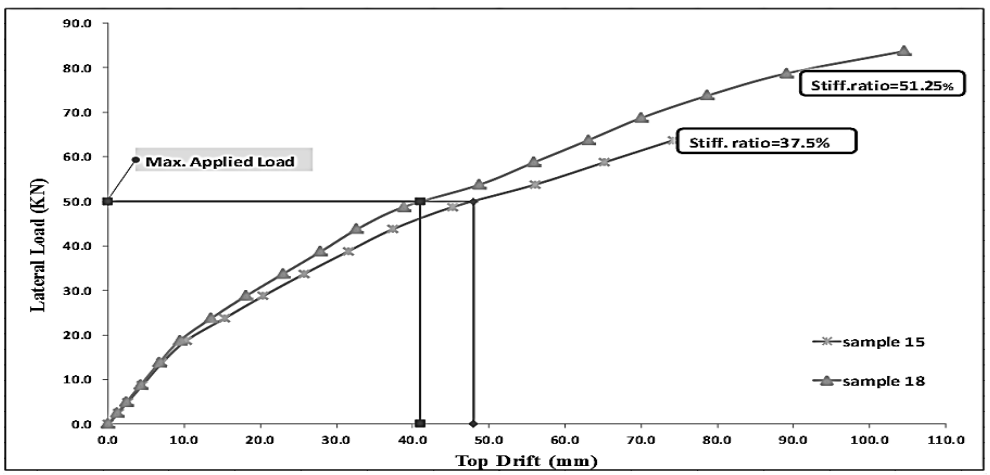

(a) The differences in the top drift value at the maximum applied horizontal load

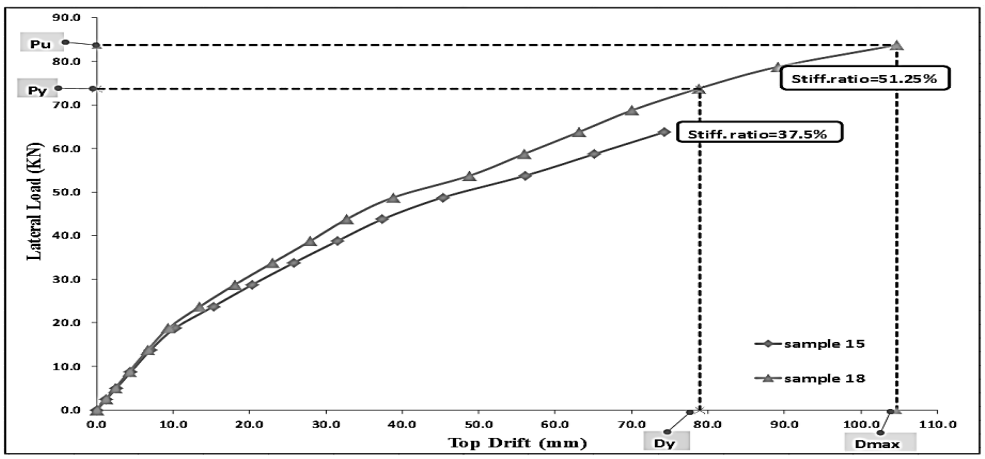

(b) The differences in the ductility ratio

Figure 14. The variation of top drift for samples 15 and 18 at different increments of loading

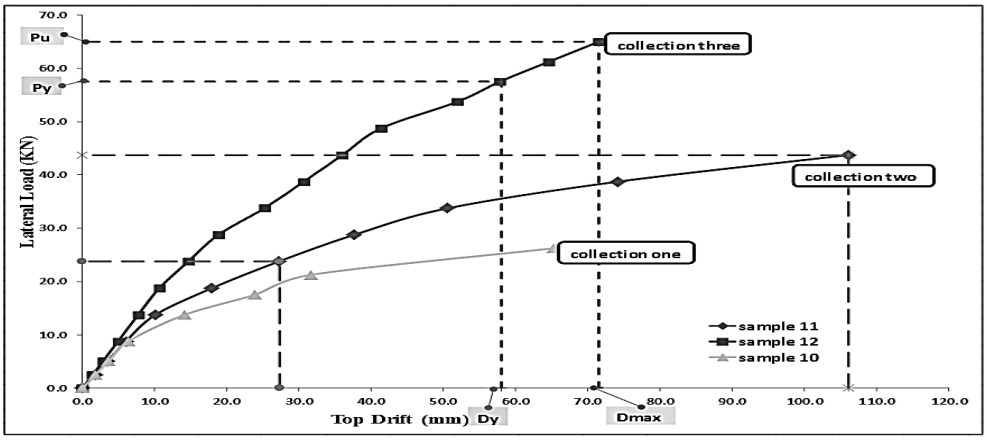

Figure 15. The variation of top drift for samples 10, 11 and 12 at different increments of loading with difference in the ductility ratio

6. CONCLUSION

According to the results obtained from the present non-linear analysis of coupled shear walls supported on two columns, the following conclusions were drawn:

1. The stress concentration mainly occurred at the whole length of the supporting columns, the junction between columns and walls, the connection between connecting beams and walls. The maximum value of stresses attained at the bottom of the supporting columns. Therefore, increasing the stiffness ratio between columns and shear walls leads to high horizontal load capacity, but with a low ratio of ductility.
2. The stiffness ratio between shear walls and supporting columns, under the effect of the lateral loads, is more crucial rather than characteristic strength and the reinforcement ratio.
3. The positions of flexural and shear cracks mainly attained at the transfer beam, the connection between connecting beams and shear walls, and the supporting columns, respectively.
4. The transfer beam and the connecting beams are crucial in the pushover analysis. Therefore, the reinforcement with proper anchorage for these elements should be detailed to avoid catastrophic failure modes.

REFERENCES

[1] A. S. Morgan, *Linear and nonlinear analysis of coupled shear walls supported on columns*, M.Sc. Thesis, Structural Engineering Department, Faculty of Engineering, Cairo University, 1992.

[2] A. A. Khaled, *Nonlinearity of coupled R.C. systems part I: Coupled shear walls supported on columns*, M.Sc. Thesis, Structure Engineering Department, Faculty of Engineering, Tanta University, 2004.

[3] Egyptian Code of Practice: ECP 203-2007, *Design and Construction of Reinforced Concrete Structure*, Ministry of Building Construction, Research Center for Housing, Building and Physical Planning, Cairo, Egypt, 2007.

[4] H. J. Pam, A. K. H. Kwan and M. S. Islam, Flexural strength and ductility of reinforced normal- and high-strength concrete beams, *Proceedings of the Institution of Civil Engineers - Structures and Buildings*, 146(4), 381–389, 2001.

[5] M. M. Kassem and F. M. Nazri, Dataset on the dynamic structural parameters of an old existing building exposed to earthquake loading before and after strengthening techniques – A case study, Lebanon, *Data in Brief*, 21, 2262–2283, 2018.

[6] B. S. Smith and A. Coull, *Tall Building Structures: Analysis and Design*, John Wiley and Sons, 1991.

[7] ANSYS user's manuals, *Structural Analysis Guide*, Release 12.0, ANSYS Inc. South Pointe 275 Technology Drive Canonsburg, PA 15317, April 2009.

[8] S. Martinez, A. H. NiIson and F. O. Slate, Spirally-reinforced high-strength concrete columns, *ACI Journal*, 81(5), 431-442, 1984.

[9] K. J. Willam and E. P. Warnke, Constitutive model for the triaxial behaviour of concrete, *Seminar on Concrete Structures Subjected to Triaxial Stresses*, Bergamo, Italy, 1974, pp. 1–30.

[10] J. K. Wight and J. G. Macgregor, *Reinforced Concrete: Mechanics and Design*, Prentice Hall (6th edition), 2011.

[11] A. Coull and B. S. Choo, Simplified elasto-plastic analysis of coupled shear walls, Proceedings of the Institution of Civil Engineers, 73(2), 365–381, 1982.

[12] S. Timoshenko and J. N. Goodier, *Theory of Elasticity*, First Edition, University of Michigan, 1933.

[13] T. N. Salonikios, Analytical prediction of the inelastic response of RC walls with low aspect ratio, *Journal of Structural Engineering*, 133(6), 844–854, 2007.

[14] A. A. EL-Fadeel, *Non-linear analysis of single coupled shear walls supported on columns*, M.Sc. Thesis, Structural Engineering Department, Faculty of Engineering, Cairo University, 2017.
[15] ACI Committee 318, *Building Code Requirements for Reinforced Concrete*, American Concrete Institute, Farmington Hill, Michigan, 2008.
[16] F. A. Tavarez, *Simulation of behavior of composite grid reinforced concrete beams using explicit finite element methods*, Master's Thesis, University of Wisconsin-Madison, 2001.

NOTATIONS

The following symbols are used in this paper:

H	The total height of shear walls measured from the level of transfer beam;
A	Summation of cross-sectional area for two walls;
I	Summation of second moment of area for two walls;
$A1$	Cross-sectional area of wall 1;
$A2$	Cross-sectional area of wall 2;
L	The distance between the center lines of two walls;
b	The clear span between two walls plus half height of connecting beam;
h	The distance between the center lines of connecting beams;
I_e	Effective second moment of area;
I_b	Second moment of area for connecting beam;
r	Reduction factor for I_b including shear deformations;
I_0	Second moment of area for transfer beam;
h_0	The total height of the supporting columns;
GA	The shearing rigidity;
λ	Cross-sectional shape factor, equal to 1.2 in the case of rectangular sections;
y	The lateral deflection, which is required to be calculated at any specified point;
w	The maximum value of the applied horizontal-triangular load;

APPENDIX

CALCULATIONS OF VERTICAL AND HORIZONTAL LOADS USING EGYPTIAN CODE OF PRACTICE "ECP-203"

1. CALCULATIONS OF VERTICAL LOADS

The assumed data are as follows:
- Live load = 400 kg/m^2
- Superimposed dead load = 150 kg/m^2
- Wall bricks weight per square meter = 150 kg/m^2
- Thickness of each slab = 220 mm

Factored vertical loads are calculated due to the weight of shear walls, coupling beams, columns, in addition to loads of slabs, as shown in the following equation:

- Total vertical factored load = 1.4 (weight of shear walls + coupling beams + columns) + 9 × area of slab within the wall zone × weight of slab
- Total vertical factored load = 1.4 ((2.5 × 4 × 25.5 × 0.5 × 2) + (4 × 0.5 × 0.6 × 2.5 × 10) + (2 × 0.5 × 1.5 × 4 × 2.5)) + 9 × 45.6 × (1.4× (0.22 × 2.5 + 0.15) + 1.6 × 0.4)
  = 1084.85 ton
- Concentrated vertical loads/story = 1084.85/9 = 120.54 ton
- Distributed vertical loads/story =120.54/12 = 10.045 t/m = 100 kN/m

2. CALCULATIONS OF HORIZONTAL LOADS

Horizontal loads which acting on the coupled system are calculated by the response spectrum analysis using ECP-203 [3], as shown in the following steps:

The assumed data as follows:
• Cairo-zone (3)
• Soil type (D)
• Total height above foundation = 29.5 m
• Important building

The total design seismic base shear (Fb) along any principal direction is given by the following equation:

$$Fb = Sd(Ti) \times \lambda \times \frac{w}{g}$$

where,
• W = Seismic weight of the whole building, is sum of the seismic weight of all floors.
• $Sd(Ti)$ = Design horizontal acceleration spectrum value which is determined by using the following expression:

$$Sd(Ti) = ag \times \gamma 1 \times S \times \frac{2.5}{R} \times \frac{TC}{T1} \times \xi \qquad \text{In case of: } Tc \leq Ti \leq T_D$$

In which,
• $T1$ = The fundamental period of vibration of the building in the direction of analysis;
• ag = The design ground acceleration;
• R = Response modification (Force Reduction) factor as a ratio between the elastic and plastic internal forces in the building, illustrated in Code Table (8.A);
• $TC, TB, TD,$ and S = illustrated in Code Table (8.3);
• ξ and $\gamma 1$ = illustrated in Code Tables (8.3) and (A.4), respectively.

2.1 Calculations of Final Horizontal Forces Acting n Each Floor Level

• Soil class D, (S = 1.8, T_b = 0.1, T_c = 0.3, T_D = 1.2, ag = 0.159, Ct = 0.05).

• $Ti = Ct\ H^{3/4} = 0.05 \times (29.5)^{\frac{3}{4}} = 0.633 < 4$ Tc = 1.2

• $Tc \leq Ti \leq T_D$

• ξ = 1.0, $\gamma 1$ = 1.4, R = 5

• $ag = 0.15 \times 9.81 = 1.4715$ m/sec^2

• $Sd(Ti) = ag \times \gamma 1 \times S \times \frac{2.5}{R} \times \frac{TC}{T1} \times \xi = 1.475 \times 1.4 \times 1.8 \times \frac{2.5}{5} \times \frac{0.3}{0.633} \times 1.0 = 0.879$

• $Fb = Sd(Ti) \times \lambda \times \frac{w}{g}$

• Wt. of floors = $(20 \times 30 \times (0.22 \times 2.5 + 0.15 + 0.15)) \times 9 = 4590$ ton

• Wt. of shear walls, columns = $2 \times 2.5 \times (0.5 \times 4) \times 29.5 = 295$ ton

• $W_{D.L} = 295 + 4590 = 4885$ ton

• $W_{L.L} = 9 \times 0.4 \times 20 \times 30 = 2160$ ton

• $W_{D.L} + 0.5 \times W_{L.L} = 5965$ ton

• $Fb = 0.879 \times 1 \times \frac{5965}{9.81} = 534.48$ ton

• $W_i = 5965/9 = 662.78$ ton/floor

• $\sum W_i H_i = 662.78\ (5.5 + 8.5 + 11.5 + 14.5 + 17.5 + 20.5 + 23.5 + 26.5 + 29.5) = 104387.85$ t.m

• $Fi = \frac{Wi\ Hi}{\sum Wi\ Hi} \times Fb$

• $Fi = \frac{662.78 \times 534.48}{104387.85} \times Hi$

• $Fi = 3.39 \times Hi$

• The final horizontal and vertical loads are illustrated as shown in Figure 2.